engineering proceedings

MDPI

Proceeding Paper

Effects of germanium or copper addition to formamidinium cesium lead triiodide perovskite crystals

Ayu Enomoto [1], Atsushi Suzuki [1], Takeo Oku [1], Sakiko Fukunishi [2], Tomoharu Tachikawa [2] and Tomoya Hasegawa [2]

[1] Department of Materials Chemistry, The University of Shiga Prefecture, 2500 Hassaka, Hikone, Shiga 522-8533, Japan
[2] Osaka Gas Chemicals Co. Ltd., 5-11-61 Torishima, Konohana-ku, Osaka 554-0051, Japan
* Correspondence: oku@mat.usp.ac.jp

Abstract: Copper (Cu) or germanium (Ge) was added to the perovskite compounds to stabilize the photoactive α-phase of formamidinium-cesium lead triiodide. The strain for the PbI_6 octahedra was relaxed by the Cu doping, which increased the displacement of formamidinium (FA) molecules, resulting in increasing the kinetic energy. The 3d orbitals of Cu were localized near the conduction band minimum and valence band maximum, which suppressed carrier diffusion resulting in lower efficiencies of the cells. The structural distortion for PbI_6 octahedra was caused by the Ge doping, which decreased the displacement of FA molecules, resulting in a decrease in the kinetic energy. Suppression of formation of photo-inactive δ-phase resulted in formation of the α-phase. Electron density distribution showed the charge transfer from Ge to iodine (I) ions, which promoted carrier diffusion from I 5p to Ge 4p orbitals. The cells doped with 12.5% Ge also provided photovoltaic properties and a single phase structure.

Keywords: germanium; copper; formamidinium; cesium; first-principles calculations; perovskite; solar cell

1. Introduction

Organic-inorganic hybrid perovskite solar cells are being studied worldwide as next-generation solar cells due to their high conversion efficiencies and easy fabrication method [1-4]. To develop commercial perovskite solar cells in the future, photovoltaic properties and long-term stability are required [5-9]. Among various types of perovskite crystals, formamidinium cesium-lead triiodide ($FA_{1-x}Cs_xPbI_3$) perovskite crystals have provided high efficiency and stability [10,11]. However, due to photo-inactive δ-phase of $FA_{1-x}Cs_xPbI_3$ perovskite crystals, optimization of compositions and formation-conditions of thin films is required [12-14]. Substitution of Pb by other elements such as Sn [15-18], Cu [19-24],[1] Co [25], Ge [26-28], or Eu [29,30], would be one of the methods to optimize the electronic and crystal structures and to improve the photovoltaic properties. For example, adding a small amount of Sn to $FA_{1-x}Cs_xPbI_3$ perovskite crystals suppressed the phase transition from the α- to δ-phase, resulting in longer carrier lifetime and smaller temperature dependence [31]. As the same group 14 element as Pb, Ge was expected to provide a potential substitute for Pb and effective to suppress the photo-inactive δ-phase [32].

The purpose of this work is to investigate the crystal structure and properties of Cu or Ge-doped $FA_{1-x}Cs_xPbI_3$ perovskite crystals from the first-principles calculations and experiments. The effects of Ge or Cu on the $FA_{1-x}Cs_xPbI_3$ crystals were investigated by X-ray diffraction (XRD), current density-voltage (*J-V*) characteristics, band structures, partial density of states (pDOS), Born–Oppenheimer molecular dynamics calculations (BOMD), and Car-Parrinello molecular dynamics calculations (CPMD).

Citation: To be added by editorial staff during production.

Academic Editor: Firstname Lastname

Published: date

2. Materials and Methods

The present perovskite solar cells were prepared by the same method as reported in the previous works [33-35]. For preparing the perovskite compound, a mixture of CH_5N_2I (FAI), CsI, PbI_2, $PbCl_2$, GeI_2, *N*-methyl-2-pyrrolidinone (NMP, 100 μL) with the desired molar ratio in *N*,*N*-dimethylformamide (DMF, 0.5 mL) was stirred at 70 °C for 24 h. For the 2% GeI_2 added device, the mole of FAI, CsI, PbI_2 and GeI_2 was adjusted to be 0.996 M (85.6 mg), 0.204 M (26.5 mg), 1.176 M (271.1 mg) and 0.024 M (3.9 mg). The perovskite solutions were spin-coated on TiO_2 with air-blow at three times [36-38]. A solution of decaphenylcyclopentasilane (DPPS, Osaka Gas Chemical, OGSOL SI-30–15) was prepared in chlorobenzene (1.0 mL) and dropped onto the perovskite layer during the last stage of the spin-coating process [39,40]. DPPS was used as a hole-transporting material to protect the cell from moisture and oxygen [41,42]. Then, the substrate was annealed at 150 °C for 10 min. All procedures were performed in air atmosphere. A gold (Au) electrode was deposited as the top electrode. The structure of the solar cells is denoted as FTO/TiO_2/perovskite/DPPS/spiro-OMeTAD/Au. The prepared cells were stored at a temperature of 22 °C and humidity below 30%.

The ab initio quantum calculations were performed using the Vanderbilt ultrasoft pseudo-potentials, scalar relativistic generalized gradient approximations and the Perdew-Burke-Ernzerhof exchange-correlation functional and density functional theory without consideration of spin-orbital coupling effect (Quantum Espresso software). The details of the calculation methods were reported in the previous works [43-45].

3. Results and discussion

3.1. First-principles calculation

First-principles calculations for Cu- or Ge-doped crystals were performed to calculate the band structures and pDOS for each system after structural optimization at 300 K. For the Cu-doped perovskite in Figure 1(a), the 5p orbitals of I atom and 3d orbitals of the Cu atom dominate near the VBM. The 6p orbitals of the Pb atom and the 3d orbitals of the Cu atom dominate near the CBM. The localization of the 3d orbital of Cu near the VBM and CBM suppressed the carrier generation and diffusion. For the Ge-doped crystals in Figure 1(b), the 6p orbital of the Pb atom and the 4p orbital of the Ge atom overlap and dominate in the conduction band. Charge transfer from 5p orbital of the I atom to 4p orbital of the Ge atom would promote carrier generation. These results indicate that Ge-doped $FACsPbI_3$ perovskite solar cells would have better photo-voltaic properties.

Perovskite cubic crystals with partial substitution of Cu or Ge at the Pb site were analyzed by the first principles CPMD calculations. After equilibrating electronic and nucleus state at 0 K, enthalpies and relaxation process of kinetic energy were calculated at 300 K. Distances from the initial positions of carbon (C) in FA, Pb, Cu, and Ge are shown in Figure 1(c). The Cu-doped crystals showed smaller deviations of the Cu atoms from their initial positions and smaller distortions for the CuI_6 octahedron. As a result, significant change is observed at the position of C in FA. On the other hand, large shift from the initial Ge position is observed for the Ge-doped crystal, resulting in the significant strain in the crystal. Then, the deviation of C positions in FA was suppressed. Differences in the strength of the bonds between the central metal and I and the orientation of the orbitals caused differences in the distortion, which would change the interaction between the FA molecule and I, changing the kinetic behavior of the FA.

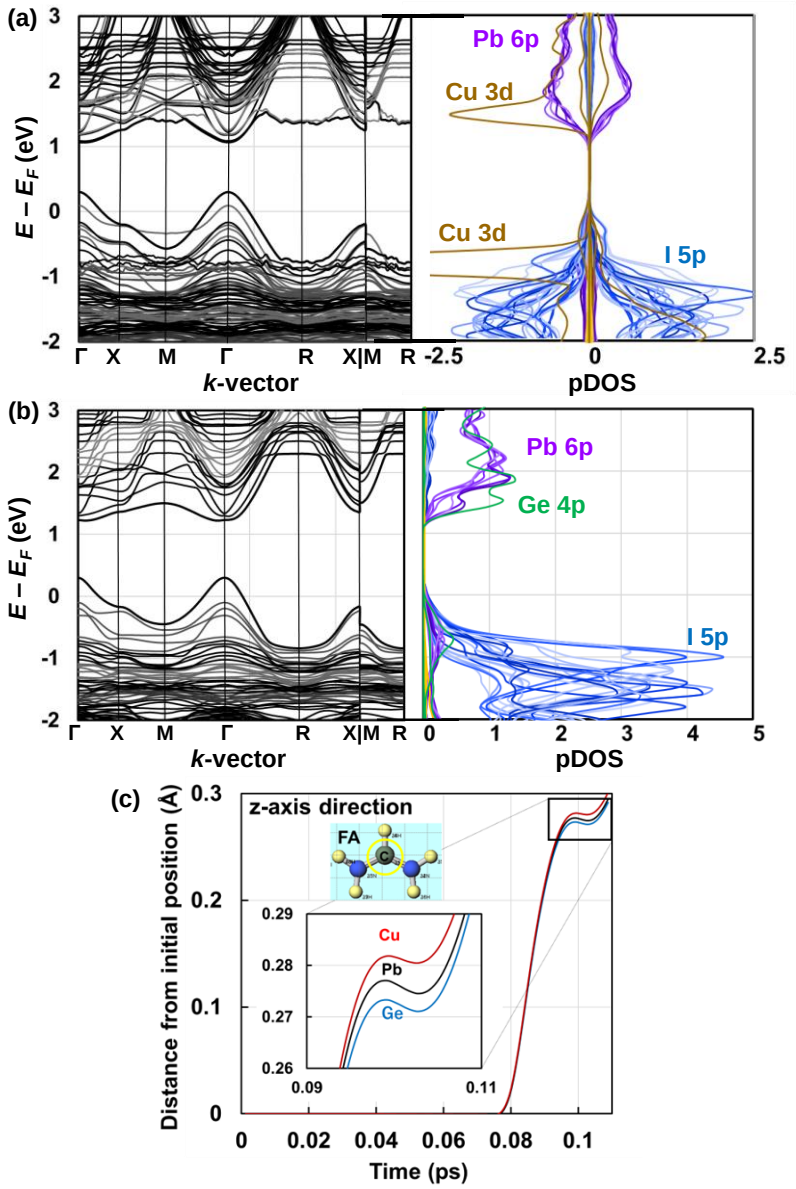

Figure 1. Calculated band structures and partial density of state of (a) $FA_{0.875}Cs_{0.125}Pb_{0.875}Cu_{0.125}I_3$ and (b) $FA_{0.875}Cs_{0.125}Pb_{0.875}Ge_{0.125}I_3$. (c) Displacements of C position in FA along z-axis.

3.2. Device characterization

$FACsPbI_3$ based perovskite solar cells added with 2% Cu, 2% Ge, 12.5% Cu, or 12.5% Ge were fabricated and characterized. XRD patterns of these cells are shown in Figure 2(a). For the device doped with 2% Cu, weak diffraction peaks of the photoactive α-phase were observed, and the photo-inactive δ-phase was formed as observed at 2θ of 12.6°. On the other hand, sharp 100 diffraction peaks of the α-phase are observed for the cells doped with 2% Ge, 12.5% Ge, and 12.5% Cu, which indicates formation of the δ-phase was suppressed, and the structure of α-phase was maintained.

J-V characteristics of the devices are shown in Figure 2(b), and the photovoltaic parameters are listed in Table 1. For the device doped with 2% Ge, J_{SC}, V_{OC} and FF were higher than those of the Cu-doped devices. When Ge was added up to 12.5%, the α-phase was formed without δ-phase, indicating Ge can be a candidate as an alternative element to Pb.

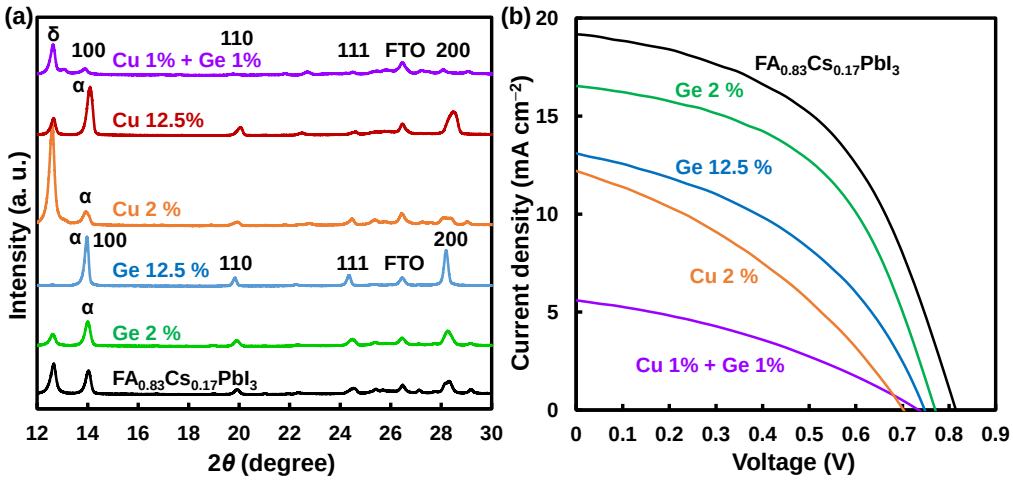

Figure 2. (a) XRD patterns of present perovskite crystals. (b) *J-V* characteristics of present solar cells.

Table 1. Photovoltaic parameters of present perovskite photovoltaic devices. J_{SC}: short-circuit current density. V_{OC}: open-circuit voltage. FF: fill factor. η: conversion efficiency.

Devices	J_{SC} (mA cm^{-2})	V_{OC} (V)	FF	η (%)
$FA_{0.83}Cs_{0.17}PbI_3$	19.3	0.815	0.496	7.74
$FA_{0.83}Cs_{0.17}Pb_{0.98}Ge_{0.02}I_3$	16.7	0.770	0.504	6.42
$FA_{0.83}Cs_{0.17}Pb_{0.875}Ge_{0.125}I_3$	13.1	0.747	0.422	4.13
$FA_{0.83}Cs_{0.17}Pb_{0.98}Cu_{0.02}I_3$	12.2	0.702	0.350	3.00
$FA_{0.83}Cs_{0.17}Pb_{0.875}Cu_{0.125}I_3$	0.583	0.0385	0.237	0.00532

4. Conclusion

In summary, the crystal structure and properties of Ge-doped FACs-based perovskite was characterized from first-principles calculations and experiments. The structural distortion for PbI_6 octahedra was caused by the Ge doping, which decreased the displacement of FA molecules, resulting in decrease of the kinetic energy. Suppression of formation of δ-phase resulted in formation of α-phase. Band structure showed the charge transfer from Ge to I ions, which promoted carrier diffusion from I 5p to Ge 4p orbitals. The perovskite solar cells doped with 12.5% Ge also provided photovoltaic properties.

Author Contributions: Conceptualization, A.E.; methodology, A.E., A.S. and T.O.; formal analysis, A.E., A.S. and T.O; investigation, A.E.; resources, S.F., T.T. and T.H.; data curation, A.E., A.S. and T.O; writing—original draft preparation, A.E., A.S. and T.O; project administration, A.E., A.S. and T.O; funding acquisition, A.S. All authors have read and agreed to the published version of the manuscript.

Funding: This research was supported by JSPS KAKENHI Grant Number JP 21K05261.

Institutional Review Board Statement: Not applicable.

Informed Consent Statement: Not applicable.

Data Availability Statement: Data is contained within the article.

Acknowledgments: The authors would like to acknowledge Dr. Takahiro Kamo, Daiichi Kigenso Kagaku Kogyo Co., Ltd, for providing CsI.

Conflicts of Interest: The authors declare no conflict of interest.

References

1. Zhang, H.; Ji, X.; Yao, H.; Fan, Q.; Yu, B.; Li, J. Review on efficiency improvement effort of perovskite solar cell. Sol. Energy 2022, 233, 421–434. https://doi.org/10.1016/j.solener.2022.01.060.
2. Sharma, R.; Sharma, A.; Agarwal, S.; Dhaka, M.S. Stability and efficiency issues, solutions and advancements in perovskite solar cells: A review. Sol. Energy, 2022, 244, 516–535. https://doi.org/10.1016/j.solener.2022.08.001
3. Park, J.; Kim, J.; Yun, H.S. Paik, M.J.; Noh, E.; Mun, H.J.; Kim, M.G.; Shin, T.J.; Seok, S.I. Controlled growth of perovskite layers with volatile alkylammonium chlorides. Nature 2023, 616, 724–730. https://doi.org/10.1038/s41586-023-05825-y.
4. Bati, A.S.R.; Zhong, Y.L.; Burn, P.L.; Nazeeruddin, M.K.; Shaw, P.E.; Batmunkh, Munkhbayar. Next-generation applications for integrated perovskite solar cells. Commun. Mater. 2023, 4, 2. https://doi.org/10.1038/s43246-022-00325-4.
5. Oku, T. Crystal structures of perovskite halide compounds used for solar cells. Rev. Adv. Mater. Sci. 2020, 59, 264–305. https://doi.org/10.1515/rams-2020-0015.
6. Meng, L.; You, J.; Yang, Y. Addressing the stability issue of perovskite solar cells for commercial applications. Nat. Commun. 2018, 9, 5265. https://doi.org/10.1038/s41467-018-07255-1.
7. Rao, M.K.; Sangeetha, D.N.; Selvakumar, M.; Sudhakar, Y.N.; Mahesha, M.G. Review on persistent challenges of perovskite solar cells' stability. Sol. Energy 2021, 218, 469–491. https://doi.org/10.1016/j.solener.2021.03.005.
8. Ueoka, N.; Oku, T.; Suzuki, A. Effects of doping with Na, K, Rb, and formamidinium cations on (CH3NH3)0.99Rb0.01Pb0.99Cu0.01I3−x(Cl, Br)x perovskite photovoltaic cells. AIP Adv. 2020, 10, 125023, https://doi.org/10.1063/5.0029162.
9. Kishimoto, T.; Oku, T.; Suzuki, A.; Ueoka, N. Additive effects of guanidinium iodide on CH3NH3PbI3 perovskite solar cells. Phys. Status Solidi A 2021, 218, 2100396. https://doi.org/10.1002/pssa.202100396.
10. Bu, T.; Li, J.; Li, H.; Tian, C.; Su, J.; Tong, G.; Ono, L.K.; Wang, C.; Lin, Z.; Chai, N.; Zhang, X.L.; Chang, J.; Lu, J.; Zhong, J.; Huang, W.; Qi, Y.; Cheng, Y.B.; Huang, F. Lead halide–templated crystallization of methylamine-free perovskite for efficient photovoltaic modules. Science 2021, 372, 1327–1332. https://doi.org/10.1126/science.abh1035.
11. Chen, S.; Pan, L.; Ye, T.; Lei, N; Yang, Y.; Wang, X. The lattice reconstruction of Cs-introduced FAPbI1.80Br1.20 enables improved stability for perovskite solar cells. RSC Adv. 2021, 11, 3997–4005. https://doi.org/10.1039/d0ra09294k.
12. Khadka, D.B.; Shirai, Y.; Yanagida, M.; Tadano, T.; Miyano, K. Interfacial embedding for high-efficiency and stable methylammonium-free perovskite solar cells with fluoroarene hydrazine. Adv. Energy Mater. 2022, 12, 2202029. https://doi.org/10.1002/aenm.202202029.
13. Jeong, J.; Kim, M.; Seo, J.; Lu, H.; Ahlawat, P.; Mishra, A.; Yang, Y.; Hope, M.A.; Eickemeyer, F.T.; Kim, M.; Yoon, Y.J.; Choi, I.W.; Darwich, B.P.; Choi, S.J.; Jo, Y.; Lee, J.H.; Walker, B.; Zakeeruddin, S.M.; Emsley, L.; Rothlisberger, U.; Hagfeldt, A.; Kim, D.S.; Grätzel. M.; Kim, J.Y. Nature 2021, 592, 381–385. https://doi.org/10.1038/s41586-021-03406-5.
14. Chen, H.; Chen, Y.; Zhang, T.; Liu, X.; Wang, X.; Zhao, Y. Advances to high-performance black-phase FAPbI3 perovskite for efficient and stable photovoltaics. Small Struct. 2021, 2, 2000130. https://doi.org/10.1002/sstr.202000130.
15. Ueoka, N.; Oku, T.; Suzuki, A.; Sakamoto, H.; Yamada, M.; Minami, S.; Miyauchi, S. Fabrication and characterization of CH3NH3(Cs)Pb(Sn)I3(Cl) perovskite solar cells with TiO2 nanoparticle layers. Jpn. J. Appl. Phys. 2018, 57, 02CE03. https://doi.org/10.7567/JJAP.57.02CE03.
16. Asakawa, Y.; Oku, T.; Kido, M.; Suzuki, A.; Okumura, R.; Okita, M.; Fukunishi, S.; Tachikawa, T.; Hasegawa, T. Fabrication and characterization of SnCl2- and CuBr-added perovskite photovoltaic devices. Technologies 2022, 10, 112. https://doi.org/10.3390/technologies10060112.
17. Luo, X.; Liu, X.; Han, L. Lead-free perovskite solar cells, what's next? Next Energy 2023, 1, 100011. https://doi.org/10.1016/j.nxener.2023.100011.
18. Macdonald, T.J.; Lanzetta, L.; Liang, X.; Ding, D.; Haque, S.A. Engineering stable lead-free tin halide perovskite solar cells: lessons from materials chemistry. Adv. Mater. 2022, 35, 2206684. https://doi.org/10.1002/adma.202206684.
19. Tanaka, H.; Ohishi, Y.; Oku, T. Effects of Cu addition to perovskite CH3NH3PbI3-xClx photovoltaic devices with hot airflow during spin-coating. Jpn. J. Appl. Phys. 2018, 57, 08RE10-1-5. https://doi.org/10.7567/JJAP.57.08RE10.
20. Ueoka, N.; Oku, T.; Suzuki, A. Additive effects of alkali metals on Cu-modified CH3NH3PbI3−δClδ photovoltaic devices. RSC Adv. 2019, 9, 24231. https://doi.org/10.1039/C9RA03068A.
21. Ueoka, N.; Oku, T. Effects of co-addition of sodium chloride and copper (II) bromide to mixed-cation mixed-halide perovskite photovoltaic devices. ACS Appl. Energy Mater. 2020, 3, 7272–7283. https://doi.org/10.1021/acsaem.0c00182.
22. Okumura, R.; Oku, T.; Suzuki, A.; Okita, M.; Fukunishi, S.; Tachikawa, T.; Hasegawa, T. Effects of adding alkali metals and organic cations to Cu-based perovskite solar cells. Appl. Sci. 2022, 12, 1710. https://doi.org/10.3390/app12031710.
23. Enomoto, A.; Suzuki, A.; Oku, T.; Okita, M.; Fukunishi, S.; Tachikawa, T.; Hasegawa, T. Effects of Cu, K and guanidinium addition to CH3NH3PbI3 perovskite solar cells. J. Electron. Mater. 2022, 51, 4317–4328. https://doi.org/10.1007/s11664-022-09688-3.
24. Suzuki, A.; Kitagawa, K.; Oku, T.; Okita, M.; Fukunishi, S.; Tachikawa, T., Additive effects of copper and alkali metal halides into methylammonium lead iodide perovskite solar cells, Electron. Mater. Lett. 2022, 18, 176–186. https://doi.org/10.1007/s13391-021-00325-5.
25. Suzuki, A.; Oe, M.; Oku, T. Fabrication and characterization of Ni-, Co-, and Rb-incorporated CH3NH3PbI3 perovskite solar cells. J. Electron. Mater. 2021, 50, 1980–1995. https://doi.org/10.1007/s11664-021-08759-1.

26. Kogo, A.; Yamamoto, K.; Murakami, T.N. Germanium ion doping of CsPbI3 to obtain inorganic perovskite solar cells with low temperature processing. Jpn. J. Appl. Phys. 2022, 61, 020904. https://doi.org/10.35848/1347-4065/ac4927.
27. Shao, J.Y.; Li, D.; Shi, J. et al. Recent progress in perovskite solar cells: material science. Sci. China Chem. 2023, 66, 10–64. https://doi.org/10.1007/s11426-022-1445-2.
28. Morteza Najarian, A.; Dinic, F.; Chen, H.; et al. Homomeric chains of intermolecular bonds scaffold octahedral germanium perovskites. Nature 2023, 620, 328–335. https://doi.org/10.1038/s41586-023-06209-y.
29. Suzuki, A.; Kishimoto, K.; Oku, T.; Okita, M.; Fukunishi, S.; Tachikawa, Additive effect of lanthanide compounds into perovskite layer on photovoltaic properties and electronic structures. Synth. Met. 2022, 287, 117092. https://doi.org/10.1016/j.synthmet.2022.117092.
30. Suzuki, A.; Oku, T. Effects of mixed-valence states of Eu-doped FAPbI3 perovskite crystals studied by first-principles calculation, Mater. Adv. 2021, 2, 2609–2616. https://doi.org/10.1039/D0MA00994F.
31. Li, R.; Song, J.; Peng, J.; Tian, X.; Xu, Y.; Huang, H.; Bai, S.; Li, Y.; Yao, F.; Lin, Q. Temperature-dependent performance metrics of tin-doped perovskite photodetectors. J. Mater. Chem. C 2022, 10, 1625–1631. https://doi.org/10.1039/D1TC05762F.
32. Enomoto, A.; Suzuki, A.; Oku, T.; Fukunishi, S.; Tachikawa, T.; Hasegawa, T. First-principles calculations and device characterizations of formamidiniumcesium lead triiodide perovskite crystals stabilized by germanium or copper. Jpn. J. Appl. Phys. 2023, 62, SK1015. https://doi.org/10.35848/1347-4065/acc6d8.
33. Taguchi, M.; Suzuki, A.; Oku, T.; Ueoka, N.; Minami, S.; Okita, M. Effects of annealing temperature on decaphenylcyclopentasilane-inserted CH3NH3PbI3 perovskite solar cells. Chem. Phys. Lett. 2019, 737, 136822. https://doi.org/10.1016/j.cplett.2019.136822.
34. Suzuki, A.; Hasegawa, R.; Funayama, K.; Oku, T.; Okita, M.; Fukunishi, S.; Tachikawa, T.; Hasegawa, T. Additive effects of CuPcX4-TCNQ on CH3NH3PbI3 perovskite solar cells. J. Mater. Sci. Materi. Electron. 2023, 34, 588. https://doi.org/10.1007/s10854-023-10001-z.
35. Terada, S.; Oku, T.; Suzuki, A.; Okita, M.; Fukunishi, S.; Tachikawa, T.; Hasegawa, T. Ethylammonium bromide- and potassium-added CH3NH3PbI3 perovskite solar cells. Photonics 2022, 9, 791. https://doi.org/10.3390/photonics9110791.
36. Oku, T.; Ohishi, Y.; Ueoka, N. Highly (100)-oriented CH3NH3PbI3(Cl) perovskite solar cells prepared with NH4Cl using an air blow method. RSC Adv. 2018, 8, 10389–10395. https://doi.org/10.1039/c7ra13582c.
37. Ono, I.; Oku, T.; Suzuki, A.; Asakawa, Y.; Terada, S.; Okita, M.; Fukunishi, S.; Tachikawa, T. Fabrication and characterization of CH3NH3PbI3 solar cells with added guanidinium and inserted with decaphenylpentasilane, Jpn. J. Appl. Phys. 2022, 61, SB1024. https://doi.org/10.35848/1347-4065/ac2661.
38. Oku, T.; Zushi, M.; Imanishi, Y.; Suzuki, A.; Suzuki, K. Microstructures and photovoltaic properties of perovskite-type CH3NH3PbI3 compounds. Appl. Phys. Express 2014, 7, 121601. https://doi.org/10.7567/APEX.7.121601.
39. Oku, T.; Taguchi, M.; Suzuki, A.; Kitagawa, K.; Asakawa, Y.; Yoshida, S.; Okita, M.; Minami, S.; Fukunishi, S.; Tachikawa, T. Effects of polysilane addition to chlorobenzene and high temperature annealing on CH3NH3PbI3 perovskite photovoltaic devices. Coatings 2021, 11, 665. https://doi.org/10.3390/coatings11060665.
40. Suzuki, A.; Taguchi, M.; Oku, T.; Okita, M.; Minami, S.; Fukunishi, S.; Tachikawa, T. Additive effects of methyl ammonium bromide or formamidinium bromide in methylammonium lead iodide perovskite solar cells using decaphenylcyclopentasilane. J. Mater. Sci. Mater. Electron. 2021, 32, 26449–26464. https://doi.org/10.1007/s10854-021-07023-w.
41. Oku, T.; Nakagawa, J.; Iwase, M.; Kawashima, A.; Yoshida, K.; Suzuki, A.; Akiyama, T.; Tokumitsu, K.; Yamada, M.; Nakamura, M. Microstructures and photovoltaic properties of polysilane-based solar cells. Jpn. J. Appl. Phys. 2013, 52, 04CR07. https://doi.org/10.7567/JJAP.52.04CR07.
42. Ogawa, C.; Suzuki, A.; Oku, T.; Fukunishi, S.; Tachikawa, T.; Hasegawa, Metallophtalocyanine used interface engineering for improving long-term stability of methylammonium lead triiodide perovskite. Phys. Status Solidi A 2023, 220, 2300038. https://doi.org/10.1002/pssa.202300038
43. Suzuki, A.; Oku, T. Electronic structures and molecular dynamics of gadolinium-doped FAPbI3 perovskite crystals. Jpn. J. Appl. Phys. 2023, 62, SK1006. https://doi.org/10.35848/1347-4065/acbec0
44. Oku, T.; Uchiya, S.; Okumura, R.; Suzuki, A.; Ono, I.; Fukunishi, S.; Tachikawa, T.; Hasegawa, T. Effects of co-addition of guanidinium and cesium to CH3NH3PbI3 perovskite solar cells. Inorganics 2023, 11, 273. https://doi.org/10.3390/inorganics11070273
45. Okumura, R.; Oku, T.; Suzuki, A.; Fukunishi, S.; Tachikawa, T.; Hasegawa, T. First-principles calculation analysis and photovoltaic properties of Cu compound added perovskite solar cells. Jpn. J. Appl. Phys. 2023, 62, SK1029. https://doi.org/10.35848/1347-4065/accaef.